# High-stability compact atomic clock based on isotropic laser cooling

Francois-Xavier Esnault,* David Holleville, Nicolas Rossetto, Stephane Guerandel, and Noel Dimarcq
*LNE-SYRTE, Observatoire de Paris, CNRS UPMC, 61 Avenue de l'Observatoire, 75014 Paris, France*
(Received 8 July 2010; published 29 September 2010)

We present a compact cold-atom clock configuration where isotropic laser cooling, microwave interrogation, and clock signal detection are successively performed inside a spherical microwave cavity. For ground operation, a typical Ramsey fringe width of 20 Hz has been demonstrated, limited by the atom cloud's free fall in the cavity. The isotropic cooling light's disordered properties provide a large and stable number of cold atoms, leading to a high signal-to-noise ratio limited by atomic shot noise. A relative frequency stability of $2.2 \times 10^{-13}\tau^{-1/2}$ has been achieved, averaged down to $4 \times 10^{-15}$ after $5 \times 10^3$ s of integration. Development of such a high-performance compact clock is of major relevance for on-board applications, such as satellite-positioning systems. As a cesium clock, it opens the door to a new generation of compact primary standards and timekeeping devices.

DOI: 10.1103/PhysRevA.82.033436 PACS number(s): 37.10.De, 42.50.Ct, 42.62.Fi, 06.20.−f

## I. INTRODUCTION

For the last 20 years, many experiments have used laser-cooled samples as atomic sources, and a variety of laser-cooling configurations have been investigated in two dimensions (2D) [1,2] and three dimensions (3D) [3–6]. Most of these schemes require a complex optical bench, sensitive beam alignment settings, very good stability of beam parameters (polarization, power imbalances), and large collimating optics. Nowadays, the complexity of these techniques is a drawback to the development and reliability of cold-atom-based metrological instruments (clocks, gyroscopes, and gravimeters). An original way to circumvent these issues is to use the isotropic light-cooling (ILC) configuration, where atoms are cooled in the disordered light field generated by an integrating sphere. The implementation of this technique is very easy and particularly robust as the effects of polarization and power imbalances are averaged. It was first demonstrated in 1992 [7] with a cylindrical diffusive material (spectralon) used to slow atomic beams of Na. Through the end of the 1990s, this simple and efficient 2D cooling configuration was used by several groups on $^{85}$Rb, Na, and Ne [8,9]. The first 3D isotropic light molasses was realized in 2001 on a Cs vapor [10] using a reflecting copper cylinder. Sub-Doppler temperatures as low as 3.5 $\mu$K have been obtained, demonstrating that Sisyphus-like cooling processes occur in a speckle field [11,12].

In this paper, we describe a simple and compact cesium clock named HORACE. Thanks to the 3D ILC technique performed inside the microwave spherical cavity, all the interactions (cooling, state preparation, microwave interrogation, and clock signal detection) take place in the same spatial region. We first explain the operation sequence, including the laser cooling and recapture process. The second part is dedicated to the study of noise impacting the detection signal. The last part describes the metrological characterization and the performance of the clock.

*Present address: NIST, Time and Frequency Division, Atomic Devices and Instrumentation group, 325 Broadway 80305 Boulder, CO USA; francois-xavier.esnault@obspm.fr

## II. OPERATION SEQUENCE OF THE HORACE CESIUM CLOCK

The HORACE clock achieves short-term stability performances of $2.2 \times 10^{-13}\tau^{-1/2}$ ($\tau$ being the integration time in seconds) comparable to most atomic fountains [13–17] with an expected long-term stability and accuracy around $10^{-15}$. The core of the HORACE clock is a spherical microwave cavity in which all the interactions are sequentially performed [18]. The cooling scheme is based on the ILC technique [7–10,19]; an 852-nm cooling light from a 100-kHz linewidth laser (as described in Ref. [20]) is directly injected in the cavity by six multimode fibers. As in an integrating sphere, the diverging beams are reflected and scattered on the optically polished cavity walls, increasing the stored light intensity. Moreover, power imbalances and polarization fluctuations of the incoming light are averaged and homogenized. To prevent degradation of the 96% reflectivity of the copper cavity walls from interaction with cesium, the vapor is enclosed in a blown quartz bulb, which is glued to the titanium vacuum chamber. For the microwave interrogation stage, the cavity is fed by two symmetric antennas and operates a cylindrical $TEM_{011}$ mode (see Fig. 1) with a microwave quality factor of $Q \approx 5000$. A key advantage of the ILC scheme in a microwave cavity is that very little optical access is required for the cooling fibers, limiting cavity phase shift. For clock signal detection, a vertical $\sigma^+ - \sigma^+$ polarized retroreflected beam probes the atomic absorption. Atomic velocity diagnostics are performed in a time-of-flight detection zone, located 9 cm below the cavity (not shown).

The typical operation sequence of the HORACE clock lasts $T_c = 80$ ms. We first laser cool Cs atoms from a room-temperature vapor (density $\sim 6 \times 10^8$ atoms cm$^{-3}$) using the isotropic light technique. We use 35 mW of cooling light tuned 10 MHz below the cycling transition ($^6S_{1/2}|F = 4\rangle \rightarrow {}^6P_{3/2}|F' = 5\rangle$) and 3 mW of repumping light ($^6S_{1/2}|F = 3\rangle \rightarrow {}^6P_{3/2}|F' = 4\rangle$). We superimpose the vertical retroreflected probe beam with the isotropic light to compensate for light losses along the vertical axis. Although it is low power and tuned to resonance ($I/I_{\text{sat}} = 0.5$, $I_{\text{sat}} = 1.1$ mW cm$^{-2}$ being the saturation intensity), we observe a factor 2.5 improvement on the total atom number when the probe beam is present. A typical loading time constant of the optical molasses is around

 

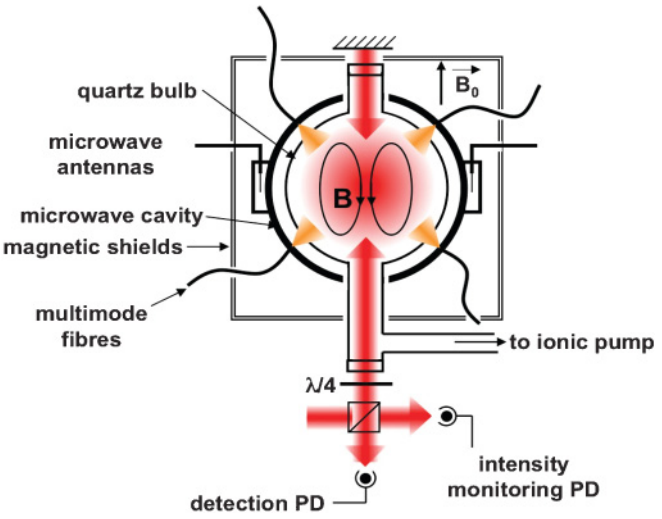


FIG. 1. (Color online) Scheme of the physics package. The two magnetic shields provide an overall attenuation of $10^3$. The vertical static field $B_0$ is 15 mG.

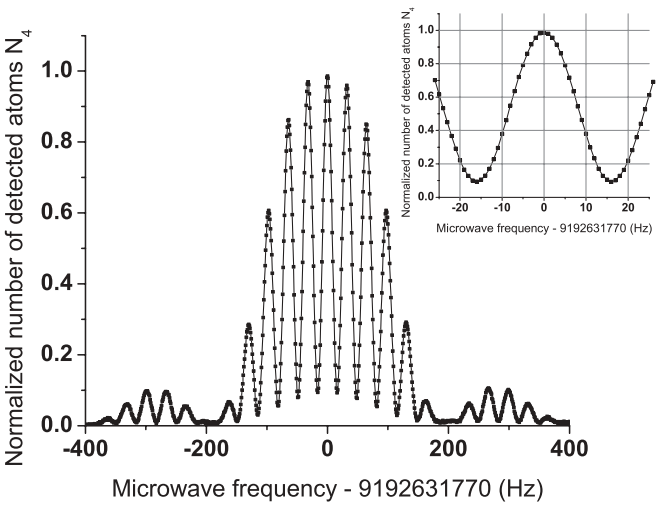


FIG. 2. Ramsey fringes of the HORACE clock. The number of detected atoms $N_4$ is plotted against the microwave frequency detuning. Inset, expanded view of the central fringe. The linewidth is $\Delta\nu = 18$ Hz, and the contrast is 90%.

80 ms. The cloud's profile can be approximated by a Gaussian distribution with a 4-mm radius at $1/\sqrt{e}$, as measured by a probe beam crossing the cavity horizontally. We estimate that only 30% of the total atom number in the cloud can be detected by the 7-mm diameter probe beam. Typically, $4 \times 10^7$ atoms are captured within the detection beam volume in $T_{\rm cool} = 40$ ms. Although parameters are set for Doppler cooling, we observe sub-Doppler atomic temperatures of $T \approx 35$ $\mu$K. Further sub-Doppler cooling can be performed in a few milliseconds by decreasing the laser intensity and shifting its frequency, leading to temperatures down to 2 $\mu$K [21]. This result indicates the existence of polarization and intensity gradients of the light pattern. Nevertheless, for ground operation, we keep the simple Doppler cooling sequence, since the thermal expansion of the cloud is not limiting clock performance. Atoms are then optically pumped into the $|F = 3\rangle$ state with the fraction of atoms in the useful clock sublevel $|F = 3, m_F = 0\rangle$ being about 20%. During the sample's free fall inside the cavity (limited by gravity to 50 ms), atoms undergo Ramsey interrogation via two 5-ms microwave pulses separated by a free evolution time of 25 ms. The resulting linewidth of the $|3,0\rangle \rightarrow |4,0\rangle$ clock transition is $\Delta\nu = 18$ Hz. The population of the $|4,0\rangle$ clock state, called $N_4$, is extracted from an absorption measurement using a 2-ms resonant 8-$\mu$W pulse of the vertical probe beam. The observed fringes are shown in Fig. 2. Successive measurements of $N_4$ on each side of the central fringe provide an error signal used to lock the mean microwave frequency with a bandwidth $f_{\rm lock}$.

A nice feature of this all-in-one-place geometry is the ability to recycle part of the cold-atom cloud from one cycle to another. Provided that the atomic free fall is not too long and the detection process does not significantly heat the atoms, a significant fraction of the cloud remains in the capture zone after the full clock cycle. When the cooling light is switched on again, the optical molasses is already partially loaded so that, for a given cooling time, the total number of cold atoms is increased. The steady-state regime of this recapture scheme is reached within 5–10 cycles. With our sequence parameters (25 ms $< T_{\rm int} <$ 35 ms), the recapture process leads to a gain factor of the cold-atom number between 1.5 and 2. In Fig. 3, we show the number of detected atoms as a function of $T_{\rm int}$ with and without recapture for a typical cooling duration of $T_{\rm cool} = 40$ ms. The improvement due to recapture is modest for on-ground operation, since the spatial overlap is small for our typical free-fall duration. However, recapture would be of major relevance in microgravity where the cold-atom cloud would remain at the center of the capture zone. In this case, the recapture efficiency would be limited by thermal expansion of the cloud.

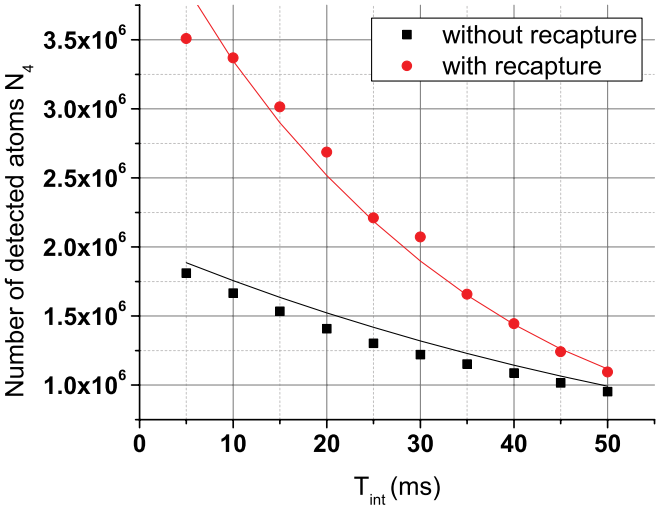


FIG. 3. (Color online) Number of detected atoms in $|F = 4, m_F = 0\rangle$ versus $T_{\rm int}$ with (●) and without (■) recapture. Lines are derived from a simple model of recapture and loss processes. Loss processes are dominated by collisions with Cs background pressure.

### III. EFFECT OF NOISE ON DETECTION SIGNAL

As far as detection goes, the clock signal is derived from the measurement of a photodetected signal called $S$, which can be written as

$$S = \eta_{\mathrm{det}} I_L e^{-N_{\mathrm{vap}}\alpha_{\mathrm{vap}}} e^{-N_4\alpha_{ca}}, \quad (1)$$

where $\eta_{\mathrm{det}}$ is the gain of the detection chain, $I_L$ is the probe laser intensity, $N_{\mathrm{vap}}$ is the number of detected atoms of the background vapor, $\alpha_{\mathrm{vap}}$ and $\alpha_{ca}$ are the mean-absorption-per-atom coefficient for a background atom and a cold-atom, respectively. The useful signal for clock operation is the cold-atom absorption $1 - e^{-N_4\alpha_{ca}}$. For a typical absorption of 2.5%, we estimate the number of atoms to be $N_4 = 1.5 \times 10^6$ with a 30% uncertainty. The absorption due to background vapor is 20%. All of the parameters in Eq. (1) are time varying and contribute to the final clock signal's relative fluctuations $\frac{\sigma_{N_4}}{N_4}$, but only the ones faster than $f_{\mathrm{lock}}$ have a significant impact. Slower fluctuations, such as thermal-induced drifts of the Cs vapor pressure and cold-atom number, are filtered by the modulation-locking technique so that the mean clock frequency is not affected. The principal relative noise sources are classified in Table I by their dependence on $N_4$. Contributions scaling as $\frac{1}{N_4}$ account for the three main technical noise sources: detection electronics, fluctuations of the detection beam intensity, and variations of background Cs vapor density. The detected signal $S$ depends on probe laser intensity. To eliminate its instrumental fluctuations, part of the detection beam is used to monitor the incoming intensity $I_L$. The ratio $S/I_L$ gives direct access to the atomic absorption. The low saturating probe beam ($I/I_{\mathrm{sat}} = 0.04$) ensures that the absorption-per-atom coefficients $\alpha_{\mathrm{vap}}$ and $\alpha_{ca}$ are independent of laser intensity. Although $N_{\mathrm{vap}}$ is eight times larger than $N_4$, the shot-noise contribution due to $N_{\mathrm{vap}}$ is smaller than the one associated with $N_4$. Since the mean transit time of thermal atoms through the probe beam is about $t_{\mathrm{vap}} = 20\ \mu$s, about 100 independent detection processes are averaged within the $T_{\mathrm{det}} = 2$ ms of detection. Thus, the resulting shot noise scales as $\sqrt{N_{\mathrm{vap}} t_{\mathrm{vap}}/T_{\mathrm{det}}}$, whereas shot noise of cold atoms is $\sqrt{N_4}$. As shown in Fig. 4, for atom numbers below $1.5 \times 10^5$, detection noise is dominated by technical noise. For larger values of $N_4$, relative fluctuations of the detected signal scale as $\frac{1}{\sqrt{N_4}}$, which is the signature of atomic shot noise. Observing this shot-noise behavior is clear evidence of the very good stability and robustness of the cooling scheme as it produces shot-noise-limited samples during several seconds. This time is much longer than $f_{\mathrm{lock}}^{-1} \approx 5T_c$, so the clock frequency stability is fundamentally limited by atomic shot noise. Thanks to this enhanced stability of the cold-atom number, we can use a simplified one-pulse detection sequence. A normalization sequence would allow us to reach the quantum projection noise limit [22,23] by getting rid of Poissonian fluctuations of the cold-atom number. Thus, the theoretical atomic noise contribution would decrease from $\frac{1}{\sqrt{N_4}}$ down to $\frac{1}{\sqrt{N_3+N_4}} \approx \frac{1}{\sqrt{2N_4}}$, but it would increase technical noise as well, as several detection pulses are required to measure both populations. Keeping in mind that simplicity is also a major goal for us, a normalization scheme would not lead to significant improvements. The two noise sources independent of detected atom number, aliasing microwave frequency noise and frequency fluctuations of the detection beam (FM-AM conversion), are not visible in Fig. 4. Nevertheless, we calculated their contributions to be both at the $2 \times 10^{-4}$ level.

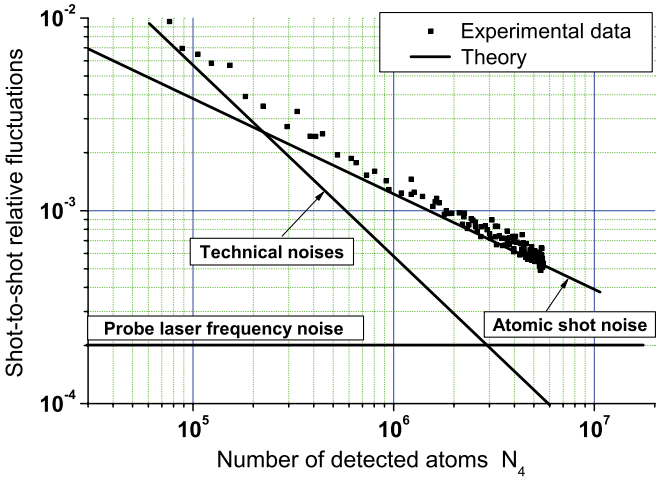


FIG. 4. (Color online) Shot-to-shot relative fluctuations of the detected signal $\frac{\sigma_{N_4}}{N_4}$ as a function of detected cold-atom number $N_4$. Here, atoms undergo an on-resonance $\pi/2$ pulse that first order cancels sensitivity to microwave frequency fluctuations but preserves other detection noise contributions.

### IV. FREQUENCY STABILITY MEASUREMENTS

The interrogation microwave field of around 9.192 GHz is synthesized from a 100-MHz signal combining the very low phase noise properties of a cryogenic sapphire oscillator (CSO)

TABLE I. Short-term noise budget. The number of detected atoms is $N_4 = 1.5 \times 10^6$, leading to an absorption signal of 2.5%.

| Noise sources | Contribution to $\frac{\sigma_{N_4}}{N_4}$ | Scaling |
|---|---|---|
| Electronics | $0.18 \times 10^{-3}$ | $N_4^{-1}$ |
| Detection laser shot noise | $0.35 \times 10^{-3}$ | $N_4^{-1}$ |
| Background vapor shot noise | $0.34 \times 10^{-3}$ | $N_4^{-1}$ |
| Atomic shot noise | $1.0 \times 10^{-3}$ | $N_4^{-0.5}$ |
| Probe laser frequency noise | $0.2 \times 10^{-3}$ | $N_4^{0}$ |
| Local oscillator frequency noise | $0.2 \times 10^{-3}$ | $N_4^{0}$ |
| Total | $1.1 \times 10^{-3}$ | |

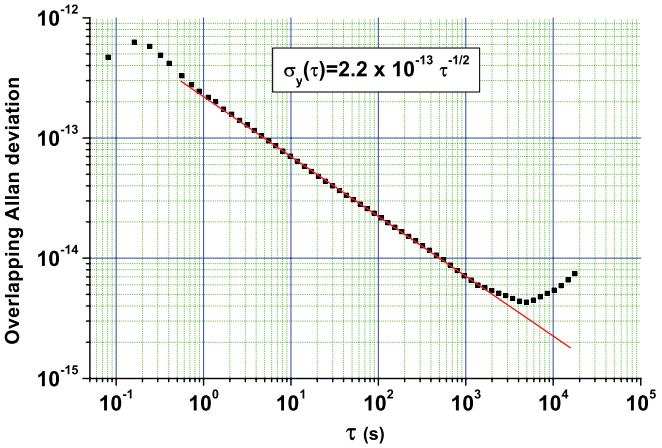


FIG. 5. (Color online) Allan standard deviation of the HORACE clock frequency measured against the CSO + H-maser.

with the long-term stability of an H-maser as described in Ref. [24]. As this reference local oscillator (LO) is much more stable than our clock, its contribution to the overall instability measurement is completely negligible. The signal-to-noise ratio (SNR) during clock operation is about 900 per cycle, leading to a short-term relative frequency stability of $2.2 \times 10^{-13}\tau^{-1/2}$. It averages as white frequency noise for 2000 s and reaches $4 \times 10^{-15}$ at 5000 s (see Fig. 5). The instability rise appearing after $5 \times 10^3$ s is under investigation and is assumed to be related to daily temperature variations. Even though noise from the LO is negligible in our laboratory due to a room-sized CSO, this is an important issue for a compact and transportable field-grade device. With a duty cycle of $T_{\rm int}/T_c = 0.45$, numerical simulations show that we can use a commercial quartz oscillator, with frequency noise $S_y(f) = 10^{-25} f^{-1} + 3.3 \times 10^{-28} f + 3.3 \times 10^{-31} f^2$ optimized for our repetition rate (12 Hz) with minor degradation. With this compact LO, the overall instability would increase from 2.2 to only $2.4 \times 10^{-13}\tau^{1/2}$.

## V. CONCLUSION

To conclude, we have shown that the ILC technique can provide a highly stable shot-noise-limited source of cold atoms with a very simple and robust experimental setup. In the framework of making an atomic clock, this stability is very advantageous, simplifying the operation sequence while keeping a high SNR. We have presented a short-term stability of $2.2 \times 10^{-13}\tau^{-1/2}$, an order of magnitude better than typical compact Rb and thermal Cs beam clocks, and close to atomic fountain performance. Systematic shifts affecting long-term operation are under investigation. As a matter of fact, the setup had been designed for short-term stability optimization, and there was no active temperature control during these measurements. Moreover, such a design can also be a versatile tool for experiments using a combination of optical and microwave pulses. Using our geometry, with a centimeter-sized collimated probe beam, let us imagine slightly modified configurations using Raman beams for atomic interferometry. We would like to point out as well that the same physics package can be used in a microgravity environment and that we expect even better performance, since recapture efficiency and interrogation time would be increased.

## ACKNOWLEDGMENTS

We thank A. Gerard, M. Lours, G. Santarelli, and A. Landragin for very precious help, and the French space agency (CNES) for supporting this work. F.X.E. acknowledges CNES and Thales Electron Devices for providing their support.

[1] W. D. Phillips and H. Metcalf, Phys. Rev. Lett. **48**, 596 (1982).
[2] K. Dieckmann, R. J. C. Spreeuw, M. Weidemuller, and J. T. M. Walraven, Phys. Rev. A **58**, 3891 (1998).
[3] H. Metcalf, *Laser Cooling and Trapping* (Springer, New York, 1999).
[4] P. Bouyer, P. Lemonde, M. B. Dahan, A. Michaud, C. Salomon, and J. Dalibard, Europhys. Lett. **27**, 569 (1994).
[5] J. M. Kohel, J. Ramirez-Serrano, R. J. Thompson, L. Maleki, J. L. Bliss, and K. G. Libbrecht, J. Opt. Soc. Am. B **20**, 1161 (2003).
[6] K. I. Lee, J. A. Kim, H. R. Noh, and W. Jhe, Opt. Lett. **21**, 1177 (1996).
[7] W. Ketterle, A. Martin, M. A. Joffe, and D. E. Pritchard, Phys. Rev. Lett. **69**, 2483 (1992).
[8] H. Batelaan, S. Padua, D. H. Yang, C. Xie, R. Gupta, and H. Metcalf, Phys. Rev. A **49**, 2780 (1994).
[9] T. G. Aardema, R. M. S. Knops, S. P. L. Nijsten, K. A. H. van Leeuwen, J. P. J. Driessen, and H. C. W. Beijerinck, Phys. Rev. Lett. **76**, 748 (1996).
[10] E. Guillot, P. Pottie, and N. Dimarcq, Opt. Lett. **26**, 1639 (2001).
[11] P. Horak, J. Y. Courtois, and G. Grynberg, Phys. Rev. A **58**, 3953 (1998).
[12] G. Grynberg, P. Horak, and C. Mennerat-Robilliard, Europhys. Lett. **49**, 424 (2000).
[13] R. Wynands and S. Weyers, Metrologia **42**, S64 (2005).
[14] D. Blonde *et al.*, Appl. Phys. B **84**, 683 (2006).
[15] J. Guena, G. Dudle, and P. Thomann, Eur. Phys. J. Appl. Phys. **38**, 183 (2007).
[16] S. Bize *et al.*, J. Phys. B **38**, S449 (2005).
[17] T. P. Heavner, S. R. Jefferts, E. A. Donley, J. H. Shirley, and T. E. Parker, Metrologia **42**, 411 (2005).
[18] F. X. Esnault, S. Perrin, S. Tremine, S. Guerandel, D. Holleville, N. Dimarcq, V. Hermann, and J. Delporte, in *Proceedings of the 2007 IEEE International Frequency Control Symposium Joint with the 21st European Frequency and Time Forum, Geneva, Switzerland, 2007* (IEEE, Piscataway, NJ, 2007), pp. 1342–1345.
[19] H.-D. Cheng, W.-Z. Zhang, H.-Y. Ma, L. Liu, and Y.-Z. Wang, Phys. Rev. A **79**, 023407 (2009).
[20] X. Baillard, A. Gauguet, S. Bize, P. Lemonde, P. Laurent, A. Clairon, and P. Rosenbusch, Opt. Commun. **266**, 609 (2006).

[21] S. Tremine, S. Guerandel, D. Holleville, J. Delporte, N. Dimarcq, and A. Clairon, in *Proceedings of the 2005 IEEE International Frequency Control Symposium and Exposition, Vancouver, BC, Canada, 2005* (IEEE, Piscataway, NJ, 2005), pp. 111–116.

[22] W. M. Itano, J. C. Bergquist, J. J. Bollinger, J. M. Gilligan, D. J. Heinzen, F. L. Moore, M. G. Raizen, and D. J. Wineland, Phys. Rev. A **47**, 3554 (1993).

[23] G. Santarelli, P. Laurent, P. Lemonde, A. Clairon, A. G. Mann, S. Chang, A. N. Luiten, and C. Salomon, Phys. Rev. Lett. **82**, 4619 (1999).

[24] D. Chambon, S. Bize, M. Lours, F. Narbonneau, H. Marion, A. Clairon, G. Santarelli, A. Luiten, and M. Tobar, Rev. Sci. Instrum. **76**, 094704 (2005).